An unsteady model for the simulation of the rapid depressurization of vessels containing two-phase mixtures in non-equilibrium conditions

Journal of Physics: Conference Series **655** (2015) 012031 doi:10.1088/1742-6596/655/1/012031

An unsteady model for the simulation of the rapid depressurization of vessels containing two-phase mixtures in non-equilibrium conditions

R Ricci[1], V D'Alessandro[1], S Montelpare[2], L Binci[1] and A Zoppi[1]

[1] Dipartimento di Ingegneria Industriale e Scienze Matematiche
Università Politecnica delle Marche
Via Brecce Bianche, 60100 Ancona (AN), Italy
[2] Dipartimento di Ingegneria e Geologia
Università degli Studi "G. D'Annuzio" di Chieti–Pescara
Viale Pindaro 42, 65127, Pescara (PE), Italy

E-mail: v.dalessandro@univpm.it

Abstract.

This paper describes the development of a simulation tool for the rapid depressurization (blowdown) of vessels containing two-phase mixtures in non–equilibrium conditions. The model adopts the cubic equations of state for fluids mixtures with non–ideal behavior for booth the phases, *i.e.* vapor and liquid, and it is based on a split two fluids model considering internal heat and mass transfer processes, as well as heat transfer with the vessel wall and the external environment. In order to account the mass and energy exchanged between the gas and the liquid phase, in conditions away from the thermodynamic equilibrium, a partial phase equilibrium (PPE) type approach has been introduced.

In this paper the validation of the proposed model with two different literature test cases is addressed and the role of the Peneloux correction for the employed equation of state is also investigated.

1. Introduction

The rapid depressurization of pressure devices is a key phenomenon in the Oil & Gas industry since it can produce a significant heat transfer between the fluid and the vessel walls. In particular the wall temperature shows a dramatic decrease and, if it falls below the ductile–brittle transition temperature of the vessel material, there is a risk for vessel wall rupture. Hence a proper vessel design needs a reliable prediction of the minimum wall and fluid temperatures that can be reached during the blowdown process [1].

It is worth noting that in some cases, starting for example from gas alone inside the vessel, the temperature drop can lead to vapor phase condensation. Moreover several experimental tests showed a significant temperature difference between the phases during and for a period after depressurization. This condition is clearly related to the greater convective heat transfer coefficient for the liquid phase (compared with the vapor one). Consequently the assumption of thermodynamic equilibrium between phases is not appropriate. At this point it is easy to understand as the matter of the numerical models development for this class of problems is a challenging task due to the complexity of the physical phenomena inside the vessel.

In the last years several numerical and experimental works with varying degrees of sophistication have been published. In particular we can find a first class of models based on simplified relations such as in [2, 3] which lead to gross over estimations. On the other hand a second group of models developed up to now, such as those proposed in [4, 5, 6, 7], is based on rigorous analytic procedures. At the time of this writing, the authors are aware only the work published by Haque in [4] as a reliable model able to take into account non–equilibrium conditions between the phases. This model provides results in good agreement with experimental data reported in [5] however is not fully documented. For this reason the main goal of this research work is the development of a reliable code for two–phase vessels blowdown. Our model treats the non–equilibrium conditions between the phases using a revisited version of the Partial–Phase Equilibrium (PPE) approach introduced in [8] and it is suitable for vessels containing one or two-phases fluids mixtures with non–ideal behavior. Peng–Robinson (PR), [9], and Soave–Redlich–Kwong (SRK), [10], equations of state (EoS) with Van der Waals mixing rules are adopted as thermodynamic model. Furthermore the Peneloux correction, [11], is also implemented for the considered EoS. This correction was introduced in order to correct liquid density predictions and it introduces a parameter influencing molar volumes and phase densities without influencing the phase equilibrium.
The code is devoted to the study of vertical and horizontal vessels considering only top vapor venting. The implemented model involves all relevant heat transfer mechanisms: internal convection, conduction through vessel wall, external convection, and it is based on a compositional approach for each phase.
The obtained results have been compared with literature experimental data, [5], as well as numerical results obtained from BLOWDOWN code reported in [1, 4, 5] showing a good agreement.

2. Governing equations

The model implemented in the code here developed is based on the assumption of non–spatial dependence of the thermodynamic quantities. In particular we use two different values of the temperature, one for the vapor, T_G, and one for the liquid, T_L, which represent the bulk temperature of each phase. For what concerns the pressure within the whole vessel it is considered uniform. This hypothesis is supported by evidence from the blowdown process occurs at a time scale which is generally much longer than the adjustment of the pressure within the vessel that occurring at the speed of sound.
Hence the proposed mathematical model is based on a system of ordinary differential equations, (ODEs), devised on the basis of mass and energy conservation laws, that can be written as:

$$\frac{\mathrm{d}\mathbf{U}}{\mathrm{d}t} = \mathbf{s}\left(\mathbf{U}\right) + \frac{\mathbf{D}}{\tau}, \tag{1}$$

where:

$$\mathbf{U} = \begin{bmatrix} n_L \\ n_G \\ n_L u_L \\ n_G u_G \end{bmatrix}, \quad \mathbf{s}\left(\mathbf{U}\right) = \begin{bmatrix} 0 \\ -\psi_{G,out} \\ q_{Lw}\mathrm{sgn}\left(n_L\right) - q_{LG} \\ q_{Gw} + q_{LG} - h_G\psi_{G,out} \end{bmatrix}, \quad \mathbf{D} = \begin{bmatrix} n_l - n_g \\ n_g - n_l \\ n_l u_l - n_g u_g \\ n_g u_g - u_l n_l \end{bmatrix}. \tag{2}$$

In eq. 1 and in eq. 2 $\mathbf{U}$ is the state vector where n_L and n_G represent the moles number of the bulk liquid and the bulk vapor phases respectively. On the other hand u_L and u_G represent the molar internal energy of each phase. Note that the internal energy is calculated as the sum of an ideal gas contribution and a residual correction depending on the non–ideal behavior:

$$u = u_{res} + \sum_{i=1}^{n_c} z_i u_i. \tag{3}$$

In eq. 3 the residual contribution u_{res} is computed on the basis of the adopted EoS, see [12], while the ideal gas contribution is found using heat capacity data applicable to gas at very low–pressure as in [13]. A similar approach is used for the enthalpy.
The entries of the source terms vector $\mathbf{s}(\mathbf{U})$ are preliminary identified in eq. 2. In particular q_{Lw} and q_{Gw} are the thermal power exchanged by convection between each phase and the vessel walls; q_{LG} is related to the heat transfer between the liquid and the vapor phases. The different heat fluxes are computed using the Newton law as follows:

$$q_{Lw} = h_{Lw} S_{Lw} \left(T_{Lw} - T_L\right), \tag{4}$$

$$q_{Gw} = h_{Gw} S_{Gw} \left(T_{Gw} - T_G\right), \tag{5}$$

$$q_{LG} = h_{LG} S_{LG} \left(T_L - T_G\right) \mathrm{sgn}\left(n_L\right). \tag{6}$$

In the previous equations S_{LG} is the area of the interface between the two phases, while S_{Lw} and S_{Gw} are the areas of the interface between the phases and the wall in contact with themselves.
Moreover the convective heat transfer coefficient between the liquid phase and vessel walls, h_{Lw}, is evaluated using the correlation suggested by Ford in [14]. The h_{Gw} coefficient, instead, is evaluated according to [15, 16] considering as reference length the vertical height of the cylinder for vertical vessels and the vessel inside diameter for horizontal axes cylinders. Lastly to calculate the convective heat transfer coefficient h_{LG}, it has been considered a plane interface between liquid and gas and the equations reported in [15] have been used.
Transport properties, *i.e.* dynamic viscosity and thermal conductivity, are computed using the corresponding states model for both the vapor and liquid mixtures, [17]. The methane transport properties are used as the reference state for the previous models and they are obtained as in [18].
The vapor phase discharge rate, $\psi_{G,out}$, appearing in eq. 2 is calculated as:

$$\psi_{G,out} = \frac{C_D \psi_{is}}{M_W^G} \tag{7}$$

where C_D is the vapor discharge coefficient fixed to a default value of 0.84, M_W^G is molar weight of the vapor while ψ_{is} is mass flow rate of an isoentropic flow through a nozzle, [19].

2.1. Partial Phase Equilibrium

The entries in "daughters phases" vector $\mathbf{D}$ in eq. 1 are evaluated using a PPE type approach which allows to take into account the non–equilibrium between the phases during the blowdown process. More in depth during the blowdown the fluid in the vessel is divided in two different zones: zone G (vapor phase) and zone L (liquid phase). In order to consider the mass and energy exchanged between the liquid and vapor phases, two new phases "g" and "l", called bubbles and droplets, respectively, are introduced. The bubbles derive from the liquid (L) vaporization while the droplets from the vapor (G) condensation. Therefore, it is assumed that the new daughter phase "g" is in phase equilibrium with the parent liquid (bulk) "L" likewise the new daughter phase "l" is in phase equilibrium with the parent gas (bulk) "G". The PPE approach here proposed fixes the instantaneous equilibrium within each partial sub–system, keeping the

initial condition of non–equilibrium between the bulk phases; in other words, it is assumed that the gas formed by vaporization (vapor) from the liquid remains instantly in equilibrium with its "parent phase" (the liquid), before mixing with the gas bulk and homogenizing with it in a time–scale τ. The same happens for the liquid. Hence the PPE approach allows to use the usual equilibrium thermodynamics, for the parent phases handling, without getting involved in the complex thermodynamics of the non–equilibrium phase change. This is certainly the key advantage of this approach.
Therefore the PPE approach allows to compute the number of moles of the droplet daughter phase, n_l, and the number of moles of vapor daughter phase, n_g, as wells as the related internal energies u_l and u_g, appearing in the vector $\mathbf{D}$, flashing in each time–step the parents phases.
The code here developed uses, for the sake of computing the entries in $\mathbf{D}$, a Vapor-Liquid Equilibria (VLE) solver for two-phase fluids mixtures. A stability analysis method is adopted, according to [20], to get better initial equilibrium coefficients, K_i for the VLE algorithm. The aim of a stability analysis is to check the thermodynamic stability of a phase. In other words if a mixture at given composition has a lower energy remaining in single phase, hence stable, or if the mixture Gibbs free–energy decreases by splitting in two or more phases, hence unstable. The modified tangent plane distance function can be safely used for this purpose and all the details about this procedure can be found in [20].
Starting from the initial estimate of the equilibrium coefficients and the feed molar composition z_i, the liquid and the vapor phases composition, x_i and y_i respectively, are generated for each parent phase introducing the overall vapor fraction β (β_G will be used in the following for vapor parent phase while β_L for liquid parent phase) according to eq. 8.

$$x_i = \frac{z_i}{1-\beta+\beta K_i}, \qquad y_i = \frac{K_i z_i}{1-\beta+\beta K_i}, \tag{8}$$

where the overall vapor fraction for each phase is obtained solving the Rachford–Rice equation:

$$g(\beta) = \sum_{i=1}^{n_c} z_i \frac{K_i - 1}{1-\beta+\beta K_i} \tag{9}$$

with $K_i \doteq y_i/x_i$.
In the VLE solver if the imbalance between the phases fugacity is not less than 10^{-9} then the K_i coefficients for G and L are updated for the iteration $(p+1)$ as follow:

$$K_i^{(p+1)} = K_i^{(p)} \left(\frac{x_i \varphi_i(\mathbf{x})}{y_i \varphi_i(\mathbf{y})} \right)^{(p)}, \tag{10}$$

where the adopted EoS is invoked to get the fugacity coefficients, φ_i. Moreover a General Dominant Eigenvalue Method (GDEM), reported in [21], was also implemented to accelerate successive substitutions method (SSM) iterations of eq. 10.
We have to remark that during the iterations the feed can be unstable even if the Gibbs free–energy increases. In particular $\Delta G/RT > 0$ if either tpd_x or tpd_y are negative:

$$\frac{\Delta G}{RT} = (1-\beta) \underbrace{\sum_{i=1}^{n_c} x_i \ln \left(\frac{x_i \varphi_i(\mathbf{x})}{z_i \varphi_i(\mathbf{z})} \right)}_{\mathrm{tpd}_x} + \beta \underbrace{\sum_{i=1}^{n_c} y_i \ln \left(\frac{y_i \varphi_i(\mathbf{y})}{z_i \varphi_i(\mathbf{z})} \right)}_{\mathrm{tpd}_y}. \tag{11}$$

In our approach the updating of equilibrium coefficient is related to Gibbs free–energy behavior; in other words, if we assume for instance $\mathrm{tpd}_y < 0$, we select K_i for the subsequent iteration as:

$$\ln K_i = \ln \varphi_i(\mathbf{z}) - \ln \varphi_i(\mathbf{y}) \tag{12}$$

otherwise if $\mathrm{tpd}_x < 0$ we use:

$$\ln K_i = \ln\varphi_i(\mathbf{x}) - \ln\varphi_i(\mathbf{z}). \tag{13}$$

The notation used up to now for the feed composition, and for its splitted phases, is obtained from the standards adopted in the Phase–Equilibria community. However in our approach we have two different feed compositions, corresponding to liquid and vapor phase, at the beginning of the specific time–step. Thus the notation is extended using a subscript which refers to a specific parent phase. Therefore the initial value for z_i is obtained from the initial conditions while in each time–step $z_{i,G}$ and $z_{i,L}$ are obtained and updated using the PPE approach as follows.
In particular in each time–step (n) we perform a VLE computation for both the parent phases (L and G) in order to compute n_l and n_g according to the following equations (obtained form eq. 8):

$$n_{l,i} = n_G^{(n)} \left(\frac{z_{i,G}}{1 - \beta_G + \beta_G K_{i,G}} \right)^{(n)} \rightarrow n_l = \sum_{i=1}^{n_c} n_{l,i}, \tag{14}$$

$$n_{g,i} = n_L^{(n)} \left(\frac{K_{i,L} z_{i,L}}{1 - \beta_L + \beta_L K_{i,L}} \right)^{(n)} \rightarrow n_g = \sum_{i=1}^{n_c} n_{g,i}. \tag{15}$$

Lastly u_l and u_g are computed invoking the EoS as in eq. 3.

2.2. Wall Temperature

In order to get T_{Lw} and T_{Gw} (the temperature of the inside vessel wall in contact with the liquid phase and the vapor phase, respectively) the 1–D Fourier equation across the vessel wall has been solved with the following boundary conditions:

$$-\lambda \left.\frac{\partial T}{\partial x}\right|_{x=0} = h_{fw}(T_{fw} - T_f) \qquad -\lambda \left.\frac{\partial T}{\partial x}\right|_{x=L_w} = h_{wa}(T_{air} - T_{wf}). \tag{16}$$

where the subscripts f refers to a generic parent phase (L or G) and L_w is the vessel wall thickness. It worth mentioning that we solve the Fourier equation, for the walls, neglecting their curvature (generally cylindrical), as we generally assume the radius of curvature to be very large, compared to the thickness. Hence we assume in first approximation as negligible the heat flux along the wall surface, compared to the heat flux across its thickness.
The Fourier equation is solved using a finite difference method with a second–order accurate central scheme for the spatial derivative while a backward Euler scheme is used for time derivative. Two ghost nodes have been introduced at the domain boundaries in order to use second–order accurate schemes also for the boundary conditions. Moreover the linear systems deriving from the implicit approach used for time integration have been solved with a standard iterative Gauss–Siedel method, [22].
The heat transfer between vessel and surrounding environment has been also considered with the coefficient h_{wa} in eq. 16. It clearly depends on the external conditions and both the natural convection and the forced convection cases have been taken into account as suggested in [16, 23].

3. Numerical Solution

The governing equations, eq. 1, are solved using a 4^{th} accurate explicit Adams-Bashfort scheme, [24], for $\mathbf{s}(\mathbf{U})$ if available three time–steps prior to the actual, otherwise lower order schemes, *i.e.* 1^{st}, 2^{nd}, or 3^{rd} are used, eq. 17. Differently for the sake of stability a first order scheme is used for the vector $\mathbf{D}$:

$$\begin{aligned}
\mathbf{U}^{(n+1)} &= \mathbf{U}^{(n)} + \Delta t \left[\frac{55}{24}\mathbf{s}^{(n)} - \frac{59}{24}\mathbf{s}^{(n-1)} + \frac{37}{24}\mathbf{s}^{(n-2)} - \frac{3}{8}\mathbf{s}^{(n-3)}\right] + \frac{\Delta t}{\tau}\mathbf{D}^{(n)} \\
\mathbf{U}^{(n+1)} &= \mathbf{U}^{(n)} + \Delta t \left[\frac{23}{12}\mathbf{s}^{(n)} - \frac{4}{3}\mathbf{s}^{(n-1)} + \frac{5}{12}\mathbf{s}^{(n-2)}\right] + \frac{\Delta t}{\tau}\mathbf{D}^{(n)} \\
\mathbf{U}^{(n+1)} &= \mathbf{U}^{(n)} + \Delta t \left[\frac{3}{2}\mathbf{s}^{(n)} - \frac{1}{2}\mathbf{s}^{(n-1)}\right] + \frac{\Delta t}{\tau}\mathbf{D}^{(n)} \\
\mathbf{U}^{(n+1)} &= \mathbf{U}^{(n)} + \Delta t\ \mathbf{s}^{(n)} + \frac{\Delta t}{\tau}\mathbf{D}^{(n)}.
\end{aligned} \tag{17}$$

We have to point out that in order to advance the solution in time, starting from the state vector $\mathbf{U}$, it is mandatory to compute the bulk temperatures, T_L and T_G, and the vessel pressure, p. For this purpose the following functions have to be defined:

$$w_L = f\left(T_L, p_L, Z_L, \mathbf{z_L}\right) - u_L, \quad w_G = f\left(T_G, p_G, Z_G, \mathbf{z_G}\right) - u_G \tag{18}$$

where Z_L and Z_G are the compressibility factors while $\mathbf{z_L}$ and $\mathbf{z_G}$ are vectors containing the molar compositions of each parent phase in a specific time–step. Hence the computation of T_L, T_G and p consists in the root finding of eq. 18 with the constraints:

$$V_0 = n_L v_L + n_G v_G, \qquad p_L = p_G. \tag{19}$$

In our code the solution of eq. 18, 19 has been achieved adopting a Newton method with Aitken acceleration, [22]:

$$T_L^{(i+1)} = T_L^{(i)} - \omega_L m_L^{(i)} \frac{w_L^{(i)}}{w_L^{\prime(i)}}, \qquad T_G^{(i+1)} = T_G^{(i)} - \omega_G m_G^{(i)} \frac{w_G^{(i)}}{w_G^{\prime(i)}} \tag{20}$$

with

$$m_L^{(i)} = \frac{T_L^{(i-1)} - T_L^{(i-2)}}{2T_L^{(i-1)} - T_L^{(i)} - T_L^{(i-2)}}, \qquad m_G^{(i)} = \frac{T_G^{(i-1)} - T_G^{(i-2)}}{2T_G^{(i-1)} - T_G^{(i)} - T_G^{(i-2)}} \tag{21}$$

note that Aitken acceleration can be introduced only when $i > 2$ hence at the beginning of the iterative algorithm a standard Newton method is used. Within each iteration (i) the pressure vessel, needed for the evaluation of w_L and w_G, is obtained by means of a further iterative loop. In particular starting from an initial guess for v_L the molar volume for vapor phase, v_G, is obtained from eq. 19 as:

$$v_G^{(j)} = \frac{V_0}{n_G^{(n)}} - \frac{n_L^{(n)}}{n_G^{(n)}} v_L^{(j-1)} \tag{22}$$

where V_0 is the vessel volume. Therefore $p_G = s\left(T_G^{(i)}, v_G^{(j)}\right)$ is computed introducing in the EoS eq. 19 and eq. 22; lastly the EoS in the Z–form is also invoked to get the compressibility factor of the liquid phase Z_L using the constraint reported in eq. 19:

$$a_3\left(p_G^{(j)}, T_L^{(i)}\right) Z^3 + a_2\left(p_G^{(j)}, T_L^{(i)}\right) Z^2 + a_1\left(p_G^{(j)}, T_L^{(i)}\right) Z + a_0\left(p_G^{(j)}, T_L^{(i)}\right) = 0 \tag{23}$$

Z_L is the minimum real root of eq. 23 and its coefficients clearly depend from the selected EoS. Thus the outer and inner loop are advanced until the quantities δ, eq. 24, and ϵ, eq. 25, are converged up to the machine precision.

$$\delta = \left| \frac{Z_L R T_L^{(i)}}{p_G^{(j)}} - v_L^{(j-1)} \right|, \tag{24}$$

$$\epsilon = \max \left(\left| \omega_L m_L^{(i)} \frac{w_L^{(i)}}{w_L^{\prime(i)}} \right|, \left| \omega_G m_G^{(i)} \frac{w_G^{(i)}}{w_G^{\prime(i)}} \right| \right). \tag{25}$$

The relaxation factors ω_L and ω_G in the following test cases are fixed to 0.1.

4. Results

In this section are presented numerical results obtained for two different test cases named S12 and HSE run3 respectively. In particular, experimental and numerical data available in [4, 5] are used as reference results for S12 problem, while numerical results available in [1] are used as reference solution for HSE run3.

It is really worth noting that time–scale τ related to the mixing between parents and daughters phases is fixed, for all the computations here reported, equal to the time–step size (its value for all the numerical tests here reported is 0.5 sec). In our computational tests stable solutions have been obtained only with this condition thus it is adopted in all the reported tests.

4.1. Case S12

The experiment S12 consists of the blowdown of a cylindrical vessel of 1.130 m diameter, 3.240 m length, 5.9 cm wall thickness and top choke of 1 cm diameter. The fluid used is a mixture of is of 66.5 mole % methane, 3.5 mole % ethane, 30.0 mole % propane. Experimental tests were performed by Haque et. al. and reported in [5]. Measured data are affected by some uncertainties such as: fluid composition and initial temperature. In particular Haque et. al. [5] provided nominal fluid compositions, meaning that, during the experiments, authors found also traces of other higher molecular weight hydrocarbons, in particular of butanes. Differently for what concerns fluid initial temperature in [5] a value ranging from 290 K to 305 K is reported in the text.

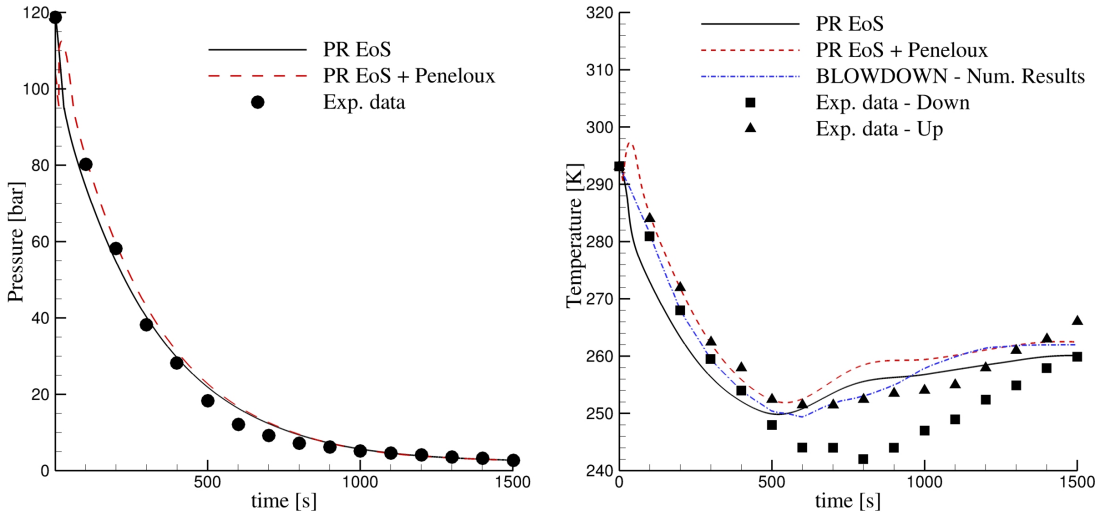

(a) Pressure (b) Vapor phase temperature

Figure 1. S12 results

In the present work we have considered an initial temperature of 293.15 K as in Fig. 8 of the reference paper [5] and the initial fluid pressure is 118.5 bar. The vessel has been considered immersed in stagnant air at 293.15 K, in equilibrium with the internal temperature as in [5]. All the computations for this test case have been performed using PR EoS with and without Peneloux correction.
Fig. 1 and Fig. 2 show the comparisons between experimental data and numerical predictions. The obtained results for the pressure evolution in the vessel, Fig. 1(a), are in excellent agreement with the experimental data. Similarly the vapor temperature predictions, Fig. 1(b), are very close to the BLOWDOWN code results, [4]. The use of Peneloux correction improves the results in the initial blowdown stage, dominated by the expansion; in the second stage the heat flux from the wall makes the vapor temperature to climb back up. However in this case the use PR equation without Peneloux corrections seems to produce results in better agreement with experimental data.
Fig. 2(a) reports the time behavior of the liquid bulk temperature. The obtained results are compared to the BLOWDOWN code and experimental data reported in [5] showing globally a good agreement. More in depth our results tend to slightly overestimate the temperature while BLOWDOWN tends to underestimates the liquid temperature.

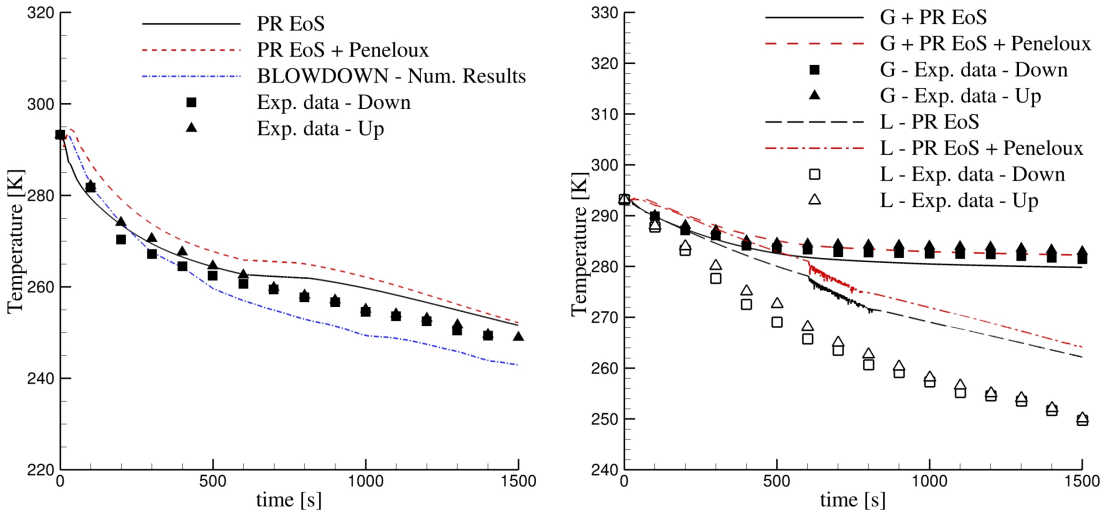

(a) Liquid phase temperature (b) Walls temperature

Figure 2. S12 results

The internal wall temperature in contact with the vapor phase is predicted very well by our code, Fig. 2(b). The use of Peneloux correction in this case seems to improve the prediction of the wall temperature at the end of the blowdown process. Instead, a reasonable agreement is observed for the liquid side which shows the same behavior of the experimental one. In this situation Peneloux volume shift produces a slight overestimation of the wall temperature.

4.2. Case HSE run3
The second test case here presented is related to numerical experiments performed by [1]. These computations were obtained on a horizontal vessel containing a mixture of hydrocarbons using BLOWFIRE code which is a fork of BLOWDOWN. The case RUN3 presented here consists of blowdown of a cylindrical vessel of 1.970 m diameter, 8.429 m length and top choke of 1.4 cm diameter with a wall thickness of 16 mm. The initial composition is of 1.0 mole % carbon dioxide,

25.0 mole % methane, 7.0 mole % ethane, 5.0 mole % propane, 4.0 mole % butane, 2.0 mole % pentane, 7.0 mole % hexane, 7.0 mole % octane, 15.0 mole % nonane and 27.0 mole % decane. As in the previous case the vessel has been considered immersed in air at 323 K and the same initial temperature of the fluid in the vessel is used. An initial molar vapor fraction of 0.83 has been considered in the performed computations while the initial fluid pressure is 22 bar. The computations have been performed using SRK EoS with and without Peneloux correction.
The results obtained using the code developed in this work are good agreement with BLOWFIRE results in terms of pressure time behavior, Fig. 3(a). In this case the adoption of Peneloux correction produces an overshoot in the pressure at beginning of the computations, while globally the pressure is slightly overestimated respect to BLOWFIRE.

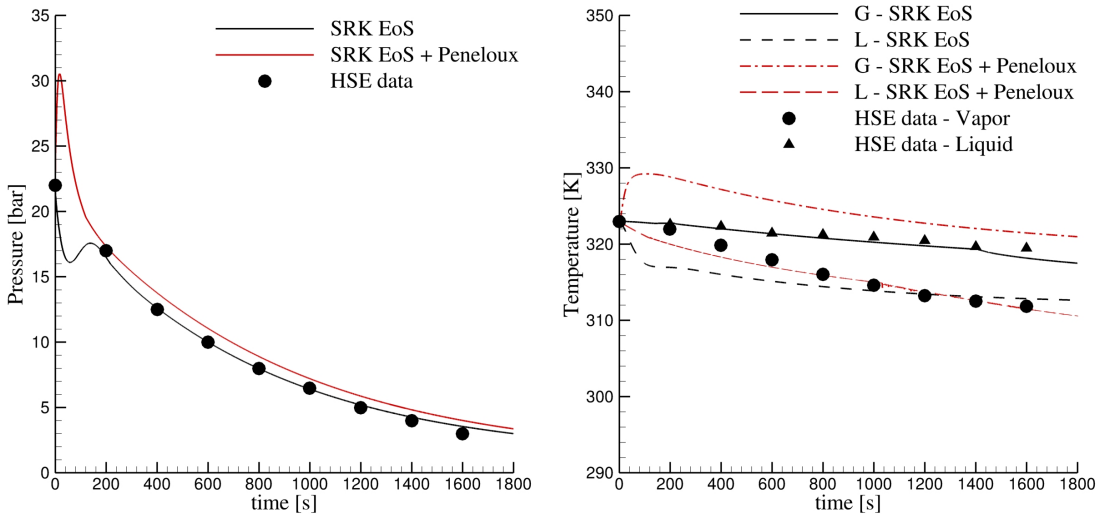

(a) Pressure (b) Walls temperature

Figure 3. HSE run3 results

Fig. 3(b) shows the predicted temperature of the wall in contact with the vapor and the liquid phases, compared with Roberts et al. [1]. Using SRK EoS without Peneloux correction the agreement is excellent for the temperature trend of the wall in contact with liquid and rather good for the temperature of the wall in contact with vapor. The temperature of the internal wall in contact with liquid phase is perfectly predicted and the temperature of the internal vessel wall in contact with vapor is underestimated at the start of the blowdown. Differently the introduction of Peneloux volume shift produces an improvement in the prediction of the wall temperature in the vapor side while in the liquid side the temperature behavior is overestimated with a different trend in time behavior.

5. Conclusions

In this work a FORTRAN code for the simulation of blowdown process of pressure vessels containing two–phase fluid mixtures has been developed. The code takes into account non–equilibrium effects, *i.e.* temperature differences between phases, using the partial phase equilibrium type approach. The proposed model has been validated comparing its results with numerical and experimental data from literature and it has showed good agreement. In particular pressure–time profiles are predicted with very good accuracy, blowdown times are estimated in line with the experiments and finally temperature–time profiles are obtained with a good accuracy by our code.

Peng–Robinson and Soave–Redlich–Kwong equations of state have been tested on two different test cases. In this work the role of Peneloux correction has been also investigated evidencing its good performance is some cases. This is probably related to the better performance of the EoS, in the liquid density prediction, obtained by introducing Peneloux correction, [25]. Lastly considering the overall performance, the code here developed produces reasonably accurate results requiring a very limited CPU time.

References

[1] Roberts T A, Medenos S and Shirvill L 2000 Review of the Response of Pressurized Process Vessels and Equipment to Fire Attack Tech. Rep. 2000-051 HSE

[2] Reynolds W C and Kays W M 1958 *Trans ASME* **80** 1160–1168

[3] Montgomery G 1995 *Hydr Proc* **4** 85–88

[4] Haque M A, Richardson S M and Saville G 1992 *Trans. Inst Chem Eng Part B* **50** 1–9

[5] Haque M A, Richardson S M, Saville G, Chamberlain G and Shirvill L 1992 *Trans. Inst Chem Eng Part B* **70** 10–17

[6] Mahgerefteh H and Wong S M A 1999 *Comp Chem Eng* **23** 1309–1317

[7] Mahgerefteh H, Gboyega B, Falope O and Oke A O 2002 *AIChE J* **48** 401–410

[8] Speranza A and Terenzi A 2005 *App Ind Math in Italy–Ser Adv Math for App Sci* **69**

[9] Peng D Y and Robinson D B 1976 *Ind Eng Chem Fund* **15** 59–64

[10] Soave G 1972 *Chem Eng Sci* **27** 1197–1203

[11] Peneloux A and Rauzy E 1982 *Fluid Phase Equilibr* **8** 7–23

[12] Michelsen M and Mollerup J M 2004 *Thermodynamic Models: Fundamentals and Computational Aspects* (Tie-Line Publications)

[13] Reid R C, Prausnitz J M and Sherwood T K 1977 *The properties of gases and liquids* (McGraw-Hill)

[14] Ford P E 1955 *4th World Petroleum Congress* (Rome–Italy)

[15] Incropera F P and Witt D D 2007 *Fundamentals of Heat and Mass Transfer* (New York: John Wiley & Sons)

[16] Churchill S W and Chu H H S 1975 *Int J Heat Mass Trans* **18** 1323–1329

[17] Pedersen K S and Fredenslund A 1987 *Chem Eng Sci* **42** 182–186

[18] Hanlet H J M, McCarty R D and Haynes W M 1975 *Cryogenics* **15** 413–417

[19] Kundu P K, Cohen I M and Dowling D R 2011 *Fluid Mechanics* (Accademic Press)

[20] Michelsen M L 1982 *Fluid Phase Equilibr* **9** 1–19

[21] Crowe A M and Nishio M 1975 *AIChE J* **21** 528–533

[22] Quarteroni A, Sacco R and Saleri F 2007 *Numerical Mathematics* (Berlin: Springer–Verlag)

[23] Sparrow E M and Gregg J L 1956 *Trans ASME* **78** 1823–1829

[24] Hairer E, Norsett S P and Wanner G 1993 *Solving ordinary differential Equations I: Nonstiff problems* (Berlin: Springer–Verlag)

[25] Pedersen K and Christensen P L 2006 *Phase Behaviour of Petroleum Reservoir Fluids* (Taylor and Francis)